Functional Disubstituted Polyacetylenes: Synthesis, Liquid Crystallinity, Light Emission, and Fluorescent Photopatterning of Biphenyl-Containing Poly(1-phenyl-octyne)s with Different Functional Bridges

Jacky W. Y. Lam,[†] Anjun Qin,[†] Yuping Dong,[†,§] Lo Ming Lai,[†] Matthias Häussler,[†] Yongqiang Dong,[†,‡] and Ben Zhong Tang*[,†,‡]

Department of Chemistry, The Hong Kong University of Science and Technology, Clear Water Bay, Kowloon, Hong Kong, China, and Department of Polymer Science and Engineering, Zhejiang University, Hangzhou 310027, China

Received: July 10, 2006; In Final Form: August 20, 2006

Biphenyl (Biph)-containing 1-phenyl-1-octynes and their polymers are synthesized, and the effects of functional bridge groups on the mesomorphic and optical properties of the polymers are studied. The nonmesomorphic disubstituted acetylene monomers $(C_6H_{13})C{\equiv}C(C_6H_4)O(CH_2)_{12}O-Biph-OC_7H_{15}$ (**1**), $(C_6H_{13})C{\equiv}C(C_6H_4)O(CH_2)_{11}$-$OOC-Biph-OC_7H_{15}$ (**2**), and $(C_6H_{13})C{\equiv}C(C_6H_4)CO_2(CH_2)_{12}OOC-Biph-OC_7H_{15}$ (**3**) are prepared by multistep reaction routes and converted into their corresponding polymers **P1**−**P3** by a WCl_6-Ph_4Sn catalyst. The structures and properties of the polymers are characterized and evaluated by NMR, TGA, DSC, POM, XRD, UV, and PL analyses. The mesogenic pendants have endowed the polymers with high thermal stability (≥400 °C). While **P1** exhibits no liquid crystallinity, **P2** and **P3** form enantiotropic S_A phase with a monolayer structure. Upon photoexcitation, the polymers emit blue and blue-green lights of 460 and 480 nm, respectively, in THF with quantum efficiencies larger than 30%. UV irradiation of a thin film of **P2** through a mask oxidizes and quenches the light emission of the exposed regions, generating a two-dimensional luminescent photoimage.

Introduction

Liquid crystals are molecular optical materials that occupy an important place in the modern optical display systems.[1] Conjugated polymers are quintessential materials for the "plastic electronics" revolution.[2] Fusing the two components into one molecular system, that is, attaching liquid-crystalline pendants to the conjugated polymer backbones, is particularly intriguing because the resulting offspring may be both light emitting and liquid crystalline, which may offer an array of exciting opportunities for high-tech innovations.

Polyacetylene is the best-known conjugated polymer, and its functionalization has attracted much attention in the past decades.[3−7] A variety of liquid-crystalline polyacetylenes have been prepared.[8−10] Almost all of them are, however, monosubstituted from the structural point of view. In comparison to the monosubstituted polymers, disubstituted polyacetylenes are superior in a number aspects; for example, they exhibit higher thermal stability, higher glass transition temperatures, and higher luminescence efficiency.[11] Creation of disubstituted liquid-crystalline polyacetylenes has, however, been a virtually unexplored area because disubstituted functional acetylenes have been difficult to polymerize.

Attracted by the potential of generating new functional polymers with enhanced and new electronic and mesomorphic properties, we decided to take the challenge. By fine-tuning the backbone rigidity and the pendant interaction through molecular engineering endeavor, we have succeeded in synthesizing mesomorphic disubstituted polyacetylenes with poly(propiolate) (**P4** and **P5**), poly(2-alkyne) [**P6**(*m*)], and poly(1-phenyl-1-alkyne) (**P7**−**P9**) skeleton structures (Chart 1).[12] We have studied their properties and acquired some information on their structure−property relationships. For example, lengthening the spacer length from four methylene units in **P6**(4) to nine units in **P6**(9) enhances the light emission efficiency and the mesogenic packing arrangements in the mesophase.[12b]

To enrich the field of liquid-crystalline disubstituted polyacetylenes and to gain more information on their structure−property relationships, in this work, we studied the effects of functional bridge groups on the properties of a group of poly(1-phenyl-1-octyne)s (PPOs) containing biphenyl mesogenic and chromophoric units (Chart 2). Unlike in **P7**−**P9**, the mesogenic pendants in **P1**−**P3** are connected to the backbone through the phenyl rings rather than the methylene spacers. Polymer **P1** with an ether bridge is found to be nonmesomorphic, whereas **P2** and **P3** with ester bridges exhibit smecticity at elevated temperatures. All the polymers emit strong lights upon photoexcitation: **P1** and **P2** are blue emitters, while **P3** emits a blue-green light. The polymers are photosensitive: UV irradiation of their solid films generates well-resolved luminescent photopatterns.

Results and Discussion

Monomer Preparation. We synthesized a disubstituted acetylene monomer 1-[4-({[(4′-heptyloxy-4-biphenylyl)oxy]-dodecyl}oxy)phenyl]-1-octyne (**1**) by a multistep reaction route (Scheme 1). We first etherified 4-iodophenol (**10**) with 1,12-

* Corresponding author. Phone: +852-2358-7375. Fax: +852-2358-1594. E-mail: tangbenz@ust.hk.
† The Hong Kong University of Science and Technology.
‡ Zhejiang University.
§ On leave from College of Materials Science and Engineering, Beijing Institute of Technology.

10.1021/jp064315y CCC: $33.50
Published on Web 09/26/2006

CHART 1

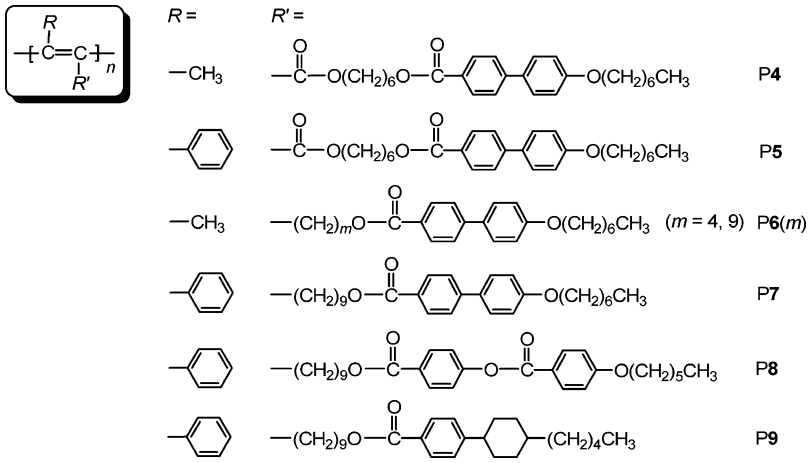

CHART 2

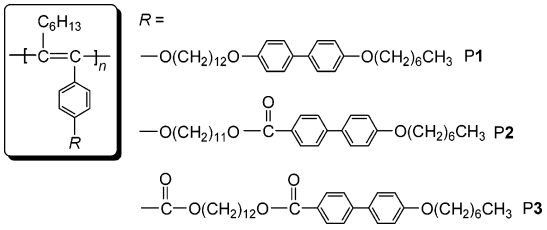

dibromodecane and then coupled the resulting product (**11**) with 1-octyne in the presence of $PdCl_2(PPh_3)_2$. The 1-phenyl-1-octyne derivative (**12**) was further etherified with 4′-hydroxy-4-biphenylyl heptyl ether (**13**), which gave the desirable monomer (**1**) in 56.4% yield (after purification by column chromatography and recrystallization). We also synthesized 1-{4-[({[(4′-heptyloxy-4-biphenylyl)carbonyl]oxy}undecyl)oxy]phenyl}-1-octyne (**2**) and 1-(4-{[({[(4′-heptyloxy-4-biphenylyl)carbonyl]oxy}dodecyl)oxy]carbonyl}phenyl)-1-octyne (**3**), which are structural cousins of **1** with different functional bridge groups, through consecutive substitution, esterification, and coupling reactions of 4-iodophenol and methyl 4-bromobenzoate (Schemes 2 and 3). All the final products, viz. the acetylene monomers, are characterized by spectroscopic methods, from which satisfactory analysis data are obtained (see the Experimental Section for details).

All the monomers are white solids at room temperature, and none of them exhibit liquid crystallinity at high temperatures. Our previous studies on the mesomorphic properties of the biphenyl-containing 1-alkynes reveal that the monomers form multifaceted mesophases.[8b,d] The nonmesomorphism of **1**−**3** suggests that the acetylene proton plays an important role in the formation of liquid-crystalline phases in the monosubstituted acetylene monomers.

Polymer Synthesis. Since the monomers are nonmesomorphic, we tried to polymerize them in the hope that the polymerization will enable the mesogenic pendants to enter the liquid-crystalline states.[13] We first investigated the catalytic activity of $NbCl_5$− and $TaCl_5$−Ph_4Sn mixtures, which are known as effective catalysts for the polymerizations of 1-phenyl-1-alkynes.[14] Stirring a toluene solution of **1** in the presence of $NbCl_5$−Ph_4Sn at 60 °C, disappointedly, gives almost no polymeric product (Table 1, no. 1). A similar result is obtained when $TaCl_5$−Ph_4Sn is used, indicating that these mixtures have little tolerance of functionality in the monomer.

We then turned our attention to $MoCl_5$− and WCl_6−Ph_4Sn mixtures. While $MoCl_5$−Ph_4Sn fails to give any polymeric product, polymerization of **1** in the presence of WCl_6−Ph_4Sn at 60 °C in toluene, delightfully, gives a polymer with a moderate molecular weight in >80% yield (Table 1, no. 4). Raising the temperature to 80 °C destabilizes the catalyst and lowers the yield dramatically. While dioxane is a good solvent for the polymerizations of monosubstituted 1-alkynes with mesogenic pendants,[8d,g] no polymeric product is isolated when we conducted the polymerization in this solvent.

Encouraged by the success in polymerizing **1** by WCl_6−Ph_4Sn, we go on to study the polymerizations of other monomers. Like **1**, monomer **2** undergoes sluggish polymerizations when $NbCl_5$−, $TaCl_5$−, and $MoCl_5$−Ph_4Sn are used as catalysts. In contrast, WCl_6−Ph_4Sn works for the polymerization at room temperature, furnishing a polymer with a high molecular weight albeit in a low yield. Raising the temperature to 60 °C does not change the yield much but decreases its molecular weight. The yield is slightly decreased at 80 °C, but the molecular weight is doubled.

The polymerization behavior of **3** is similar to that of **2**. Whereas $NbCl_5$−, $TaCl_5$−, and $MoCl_5$−Ph_4Sn are again inactive, WCl_6−Ph_4Sn can initiate the polymerization of **3** at elevated temperatures. In comparison with those in the syntheses of **P7**−**P9**,[12b,c] the results here are much poorer. Attachment of mesogenic pendant to the 1-phenyl-1-octyne structure through the phenyl ring generates sterically more bulky monomers, making them more difficult to be polymerized into high molecular weight polymers in high yields by the W-based catalyst.

Structural Characterization. We characterized the molecular structures of the polymers by standard spectroscopic methods and obtained satisfactory data corresponding to their molecular structures (see the Experimental Section for details). Since the IR spectra of the monomers show no characteristic C≡C stretching vibrations at ∼2200 cm^{-1}, we are not going to discuss the IR spectra of their polymers. Analysis by NMR spectroscopy reveals that the acetylene triple bonds of the monomers have been converted to the polyene double bonds of the polymers by the acetylene polymerization. An example of the ^1H NMR spectrum of polymer **P3** along with that of its monomer **3** is given in Figure 1. The ethynylphenyl protons of **3** resonate at δ 7.94 and 7.54, which are upfield-shifted after the monomer has been polymerized. No other unexpected signals are observed, and all the resonance peaks can be readily assigned. The NMR spectral analysis thus confirms that the molecular structure of the polymeric product is indeed **P3**, as shown in the Chart 1.

Figure 2 shows the ^{13}C NMR spectra of polymer **P3** and its

SCHEME 1

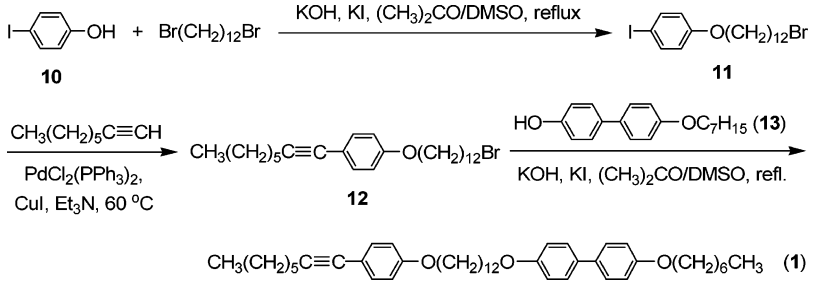

SCHEME 2

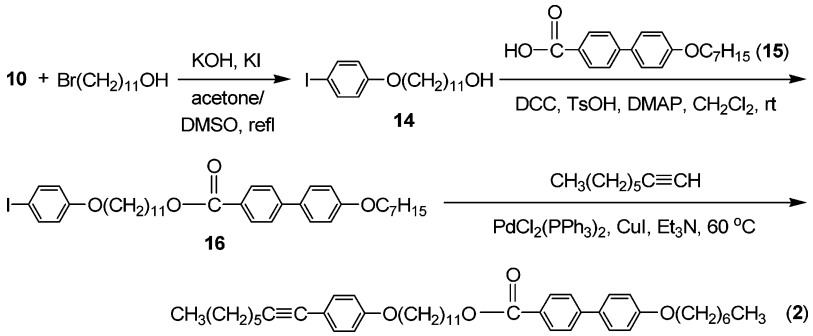

SCHEME 3

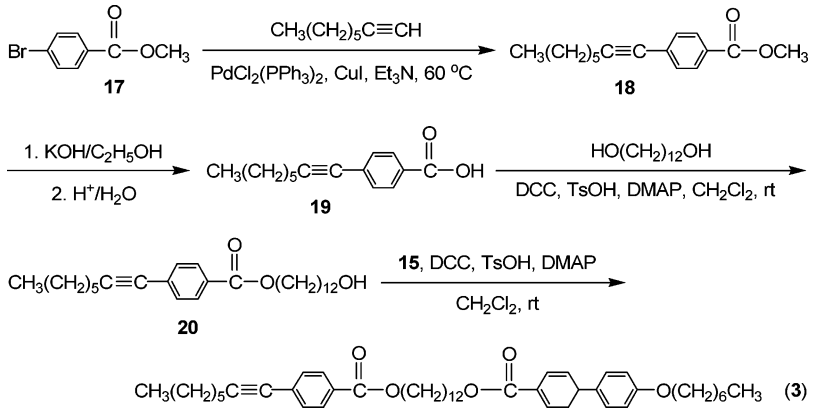

TABLE 1: Polymerization of 1-[4-({[(4′-Heptyloxy-4-biphenylyl)oxy]dodecyl}oxy)phenyl]-1-octyne (1)[a]

no.	catalyst	solvent	temp (°C)	yield (%)	M_w[b]	M_w/M_n[b]
1	$NbCl_5-Ph_4Sn$	toluene	60	trace		
2	$TaCl_5-Ph_4Sn$	toluene	60	trace		
3	$MoCl_5-Ph_4Sn$	toluene	60	0		
4	WCl_6-Ph_4Sn	toluene	60	86.4	25000	1.6
5	WCl_6-Ph_4Sn	toluene	80	51.8	30000	2.4
6	WCl_6-Ph_4Sn	dioxane	60	0		

[a] Carried out under nitrogen for 24 h; $[M]_0 = 0.2$ M, [cat.] = [cocat.] = 10 mM. [b] Determined by GPC in THF on the basis of a polystyrene calibration.

monomer **3**. While the acetylenic carbon atoms of **3** resonate at δ 90.6 and 80.0, these peaks are absent in the spectrum of **P3**. The resonance peaks of the ethynylphenyl and propargyl carbon atoms next to the triple bond at δ 131.2, 129.1, 129.0, 128.7, and 19.3 are not observed owing to their respective transformations to the styrenic and allylic structures in the polymer. The resonances of the olefinic carbon atoms in the polyene backbone are hard to assign, due to their overlap with those of the biphenyl pendants.

Thermal Stability. Since the formation of mesophases of thermotropic liquid crystals is realized by the application of heat, the thermal stability of the polymers is thus of primary concern. As can be seen from Figure 3, all the polymers enjoy good thermal stability. The thermal gravimetric analysis (TGA) thermograms show that the polymers start to lose their weights at a temperature as high as ~400 °C. Poly(1-phenyl-1-propyne) is a parent form of the polymers synthesized in this study, which loses 5% of its weight at 330 °C.[11a,15] The incorporation of biphenyl rings into the poly(1-phenyl-1-alkyne) structure has clearly enhanced the resistance of the polymer to thermolysis. The biphenyl pendants may have well wrapped the polyacetylene backbones and thus protect them from the attack by the degradative species. Analyses of the polymer samples stored under ambient temperature in open air for more than 4 years by gel permeation chromatography (GPC) find no changes in their molecular weights, indicative of their outstanding environmental stability.

Liquid Crystallinity. After confirming the thermal stability of the polymers, we investigated their thermal transitions by differential scanning calorimetry (DSC). Polymer **P1** does not show any phase transition signals during the cooling and heating cycles. Under the observation by polarized optical microscope (POM), the isotropic liquid between the glass slides remains

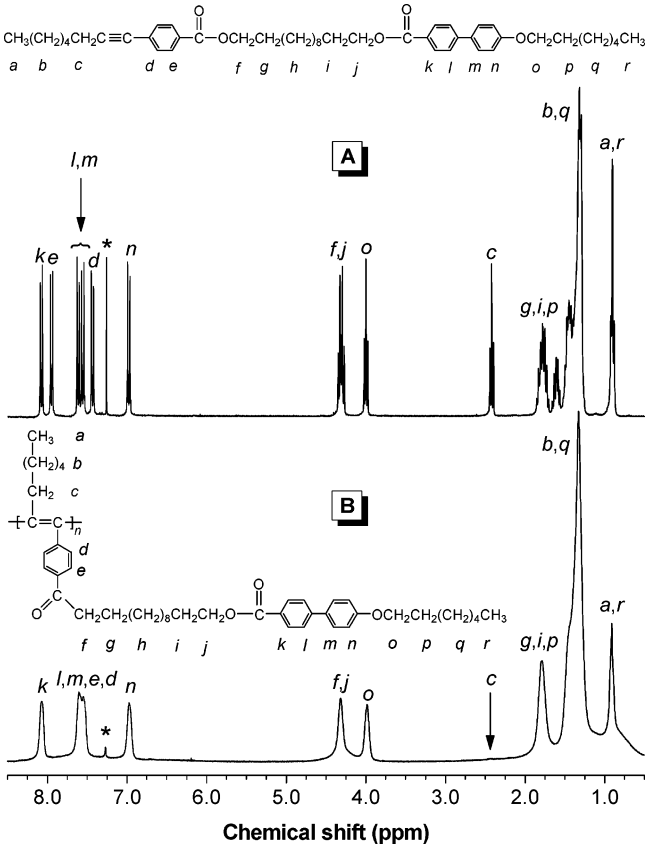

Figure 1. ^{1}H NMR spectra of (A) monomer **3** and (B) its polymer **P3** (sample from Table 2, no. 8) in chloroform-*d*. The solvent peaks are marked with asterisks.

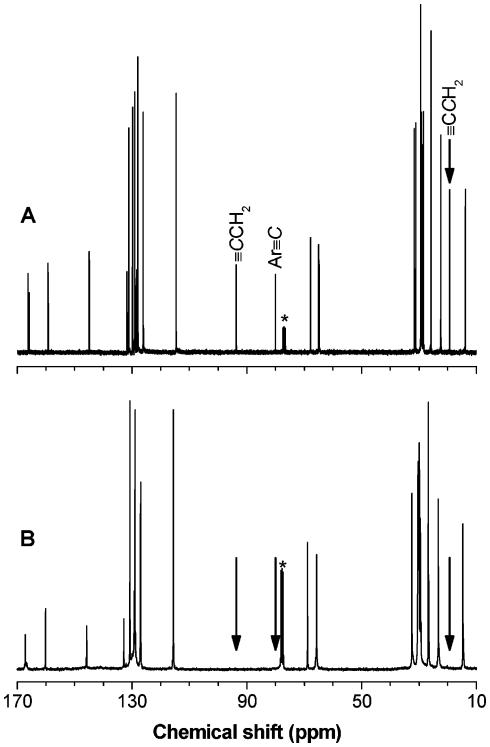

Figure 2. ^{13}C NMR spectra of (A) monomer **3** and (B) its polymer **P3** (sample from Table 2, no. 8) in chloroform-*d*. The solvent peaks are marked with asterisks.

dark even when it is cooled to solid state, in which the coverslip cannot be sliding. When the pendant functional bridge is changed from ether in **P1** to ester in **P2** and **P3**, liquid-crystalline phases are readily formed.

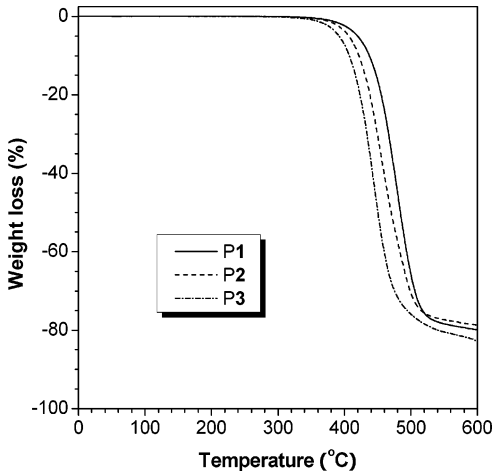

Figure 3. TGA thermograms of **P1** (sample from Table 1, no. 3), **P2** (Table 2, no. 5), and **P3** (Table 2, no. 8) recorded under nitrogen at a heating rate of 20 °C/min.

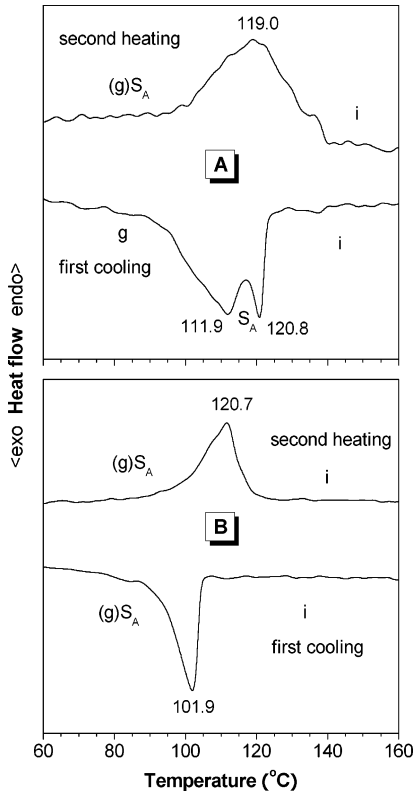

Figure 4. DSC thermograms of the mesomorphic polyacetylenes (A) **P2** (sample from Table 2, no. 5) and (B) **P3** (Table 2, no. 8) recorded under nitrogen during the first cooling and second heating scans at a scan rate of 5 °C/min. Abbreviations: g = glassy state, S_A = smectic A phase, and i = isotropic state.

The DSC thermograms of **P2** and **P3** recorded under nitrogen during the first cooling and second heating scans are shown in Figure 4. In the first cooling cycle, **P2** enters the smectic A (S_A) mesophase at 120.8 °C. The temperature range of the mesophase is narrow (~10 °C), and the polymer completely solidifies at ~110 °C. The rigid polyene backbone may have distorted the packing arrangements of the mesogenic pendants, which has in turn decreased the stability of the S_A mesophase and narrowed the mesomorphic temperature range. Although only one peak is observed at 119.0 °C in the second heating

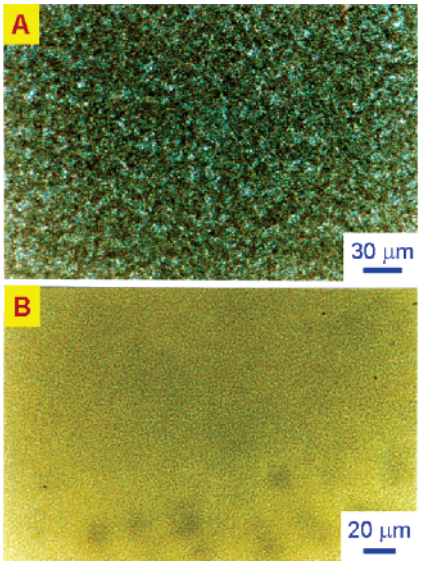

Figure 5. Mesomorphic textures observed on cooling (A) **P2** (sample from Table 2, no. 5) to 115 °C and (B) **P3** (Table 2, no. 8) to 105 °C from their isotropic melts.

cycle, mesomorphic texture is readily observed under POM, indicative of the enantiotropic nature of the mesophase.

The thermal transition profiles of **P3** are similar to those of **P2**. Its isotropic (i)−S_A and S_A−i transitions occur at 101.9 and 120.7 °C, respectively. It is noteworthy that the difference between the temperatures detected during the heating and cooling scans is very small (<1 °C). Most of the rigid PPO segments may have maintained their conformations in the neighborhood of the mesogen liquation temperatures, and the ordering of the mesogenic pendants thus can be realized by a small extent of supercooling.

Figure 5 shows the POM micrographs of the mesomorphic textures of **P2** and **P3**. When **P2** is cooled from the isotropic state, many anisotropic entities are emerged from the dark background, but their developments into a typical S_A texture are difficult. The mesogenic pendants may have still coupled with the rigid polyene backbone even when they are separated by a long alkyl spacer. It is thus difficult for the mesogens to pack and to further grow into the typical anisotropic S_A texture. The texture obtained in **P3** system is even worse, with only small-sized grains observed in the micrograph.

The thermal transitions of **P2** and **P3** and their associated enthalpy and entropy changes are listed in Table 3. The large ΔH and ΔS changes involved in the phase transitions support the assignment of smecticity to the mesophases of the polyacetylene liquid crystals because those involved in nematic transitions are much smaller.[16]

We carried out powder X-ray diffraction (XRD) experiments with the aim of collecting more information on the mesomorphic structures of the polymers and the molecular packing arrangements within the liquid-crystalline phases. The XRD diffractogram of **P2** shows a sharp reflection at $2\theta = 2.4°$ (Figure 6), from which a d-spacing of 36.78 Å is derived by the Bragg law $2d \sin \theta = n\lambda$ (Table 3). The existence of this long-range order in the polymer rules out the possibility of nematic classification and reinforces the smectic assignment.[17] The calculated length of one monomer repeat unit of **P2** at its most extended conformation is 41.08 Å, which is in excess of the experimentally obtained layer thickness. This is understandable because it is difficult or impossible for the aliphatic alky chains to adopt a fully extended conformation. The d_1/l ratio is 0.90, suggesting that the mesogenic pendants of **P2** are packed in a monolayer structure. Interestingly, the second reflection at $2\theta = 4.15°$ is readily detected by the diffractometer with a much stronger intensity. Similar phenomena have been observed in other systems although we do not know the cause for this at present.[18] The peak centered at $2\theta = 20.79°$ corresponds to the distance between the mesogenic pendants within the layer.

Similarly, **P3** shows Bragg reflections at both low- and high-angle regions, from which d-spacing corresponding to a monolayer structure can be derived. The intensity of the lowest-angle peak is, however, weak, demonstrative of a much poorer layer packing arrangements in this system, in full agreement with the DSC and POM observations.

Electronic Absorption. The absorption spectra of the polymers are given in Figure 7. Polymer **P1** exhibits a strong K-band of the biphenyl chromophore at 268 nm. Its polyene backbone absorptions occur at ~300 nm and well extend to >400 nm. Such a wide absorption region is not surprising, taking into account that conjugated polymers generally possess segments with different lengths of electronic conjugation. The absorption of its Z conformers may have overlapped with that of its E cousins, which may have also contributed to the wide absorption. The absorptivities are rather low, revealing that the bulky pendant groups have twisted the alternating double bonds and hence reduced the conjugation length along the polyene backbone.

The backbone absorptions of **P2** and **P3** are found in the similar wavelength region. Their pendants absorb at ~296 nm, which are ~28 nm red-shifted from that of **P1**. This can be understood from the structural difference of the mesogenic chromophores. The biphenyl chromophores of **P2** and **P3** are well polarized by the push−pull interaction of the electron-donating heptyloxy and the electron-accepting carbonyloxy groups. On the other hand, in **P1**, both heptyloxy and ether groups are electron-donating, which still polarize the biphenyl chromophores but to a much lesser extent.

Light Emission. Poly(1-phenyl-1-alkyne)s $-[(C_6H_5)C{=}C(CH_2)_mCH_3]_n-$ with long methylene spacers are strong emitters. PPO and **P7**, for example, emit strong blue light of ~458 nm in THF in quantum yields (Φ_F) of 43% (Figure 8) and 59%, respectively.[12a,b] The long alkyl spacers may have better segregated the polymer strands, which effectively hampers the excitions from traveling to the quenching sites and hence enhances their chances to decay radiatively. Our polymers are basically PPO derivatives carrying biphenyl chromophores. It is thus of interest to examine how the structural variations in the polymers affect their light-emitting behaviors.

Upon photoexcitation at 361 nm, **P1** emits a blue light of 463 nm (Figure 8). Its emission intensity is comparable to that of PPO, but its Φ_F (34%) is lower than those of PPO and **P7**. The emission band is broad, probably due to the variation in the conjugation length (vide supra). No photoluminescence (PL) peak from the biphenyl chromophores is detected at ~370 nm. As the PL spectrum of the biphenyl pendant overlaps with the absorption spectrum of the polyene backbone, the excitonic energy of the pendant is likely transferred to the backbone. When the pendant functional bridge group is changed from ether in **P1** to ester in **P2**, the PL peak of **P2** is found at 462 nm with a similar efficiency (33%). There seems little correlation between the Φ_F value and the polarizability of the mesogenic pendants.

Interestingly, **P3** emits a redder light with a higher intensity. Its Φ_F is, however, similar to those of **P1** and **P2**. In our previous studies, we have also observed red-shifted emissions in PPO

TABLE 2: Polymerizations of Biphenyl-Containing 1-Phenyl-1-octynes[a]

no.	catalyst	temp (°C)[b]	yield (%)	M_w[c]	M_w/M_n[c]
	1-{4-[({[(4′-Heptyloxy-4-biphenylyl)carbonyl]oxy}undecyl)oxy]phenyl}-1-octyne (**2**)				
1	$NbCl_5-Ph_4Sn$	60	0		
2	$TaCl_5-Ph_4Sn$	60	0		
3	$MoCl_5-Ph_4Sn$	60	0		
4	WCl_6-Ph_4Sn	rt	19.0	53300	1.8
5	WCl_6-Ph_4Sn	60	19.2	30400	2.0
6	WCl_6-Ph_4Sn	80	14.8	103100	2.8
	1-(4-{[({[(4′-Heptyloxy-4-biphenylyl)carbonyl]oxy}dodecyl)oxy]carbonyl}phenyl)-1-octyne (**3**)				
7	WCl_6-Ph_4Sn	rt	trace		
8	WCl_6-Ph_4Sn	60	26.2	8200	1.8
9	WCl_6-Ph_4Sn	80	19.0	8300	1.8

[a] Carried out under nitrogen in toluene for 24 h; $[M]_0 = 0.2$ M, [cat.] = [cocat.] = 10 mM. [b] rt = room temperature. [c] Determined by GPC in THF on the basis of a polystyrene calibration.

TABLE 3: Thermal Transitions and X-ray Diffraction Analysis Data of P2 and P3[a,b]

	DSC						
	T, °C [Δ*H*, kJ/mru; Δ*S*, J/(mru K)][c]						
polymer	cooling			heating			
P2	i 120.8 S_A 111.9 (−8.04; −20.59)[d] g			(g)S_A 119.0 (8.24; 21.02)[d] i			
P3	i 101.9 (−7.48; −19.95)[d] S_A(g)			(g)S_A 111.6 (8.58; 22.31)[d] i			
	X-ray Diffraction						
polymer	*T* (°C)	d_1 (Å)	d_2 (Å)	d_3 (Å)	*l* (Å)[e]	d_1/l	phase
P2	115	36.78	19.19	4.34	41.08	0.90	S_A
P3	105	40.12	20.53	4.33	46.72	0.86	S_A

[a] Data taken from the DSC thermograms recorded under nitrogen in the first cooling and second heating scans. Abbreviations: g = glassy state, S_A = smectic A phase, and i = isotropic liquid. [b] The mesomorphic structures in the liquid-crystalline states at the given temperatures are frozen by the rapid quenching with liquid nitrogen. [c] Abbreviation: mru = monomer repeat unit. [d] Overlapping transitions. [e] *l*: calculated from the monomer repeat units in their fully extended conformation.

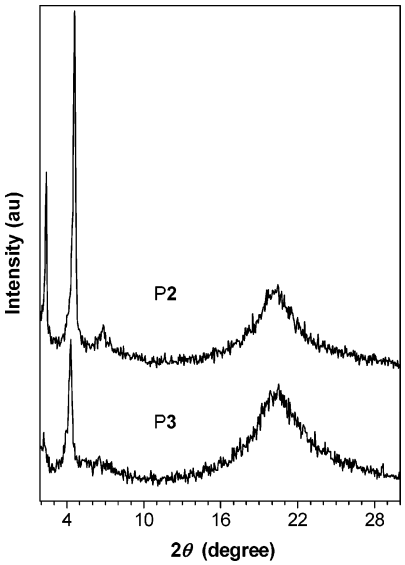

Figure 6. X-ray diffraction patterns of the mesomorphic polyacetylenes quenched with liquid nitrogen from their liquid-crystalline states: **P2** (sample from Table 2, no. 5) at 115 °C and **P3** (Table 2, no. 8) at 105 °C.

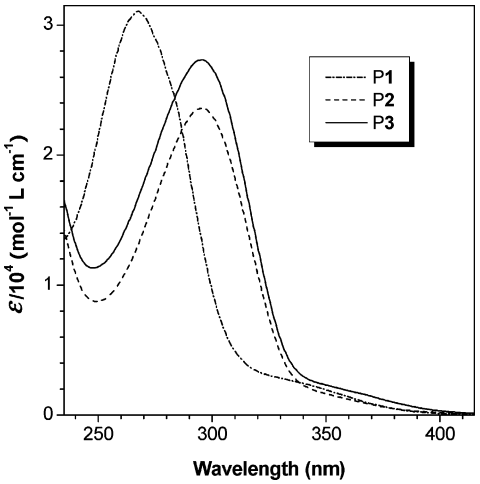

Figure 7. UV spectra of THF solutions of **P1** (sample from Table 1, no. 3), **P2** (Table 2, no. 5), and **P3** (Table 2, no. 8).

derivatives with (1*R*,2*S*,5*R*)-(−)-menthol and (1*S*-endo)-(−)-borneol pendant groups attached to the backbone phenyl rings through ester linkages.[5b,19] We believed that the ester groups have electronically perturbed the phenyl rings, which in turn alters the PL behaviors of the PPO skeleton.

Fluorescence Photopatterning. We have found that when poly(1-phenyl-1-alkyne)s are irradiated by UV light in air, their emissions are quenched due to photooxidation of the polymer chains.[5a,20] Since the polymers synthesized in this project are also emissive, we explored their potential use as PL imaging materials. The polymers can form uniform, tough films by spin-coating their solutions. UV irradiation of a thin film of **P2** through a mask bleaches the exposed regions, while the unexposed regions remain emissive. A photopattern is thus generated without performing the development process (Figure 9).

Conclusions

In this work, we synthesized a group of new biphenyl-containing PPO derivatives and studied their thermal, mesomorphic, light-emitting, and photopatterning properties. Our results and findings can be summarized as follows:

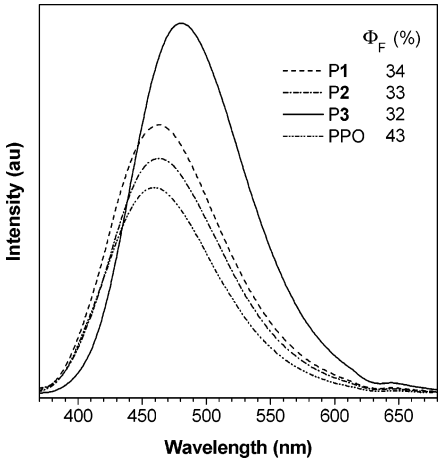

Figure 8. Photoluminescence spectra of THF solutions of **P1** (sample from Table 1, no. 3), **P2** (Table 2, no. 5), **P3** (Table 2, no. 8), and poly(1-phenyl-1-octyne) (PPO). Concentration: 0.05 mM. Excitation wavelengths (nm): 361 (**P1** and **P2**), 365 (**P3**), and 355 (PPO).

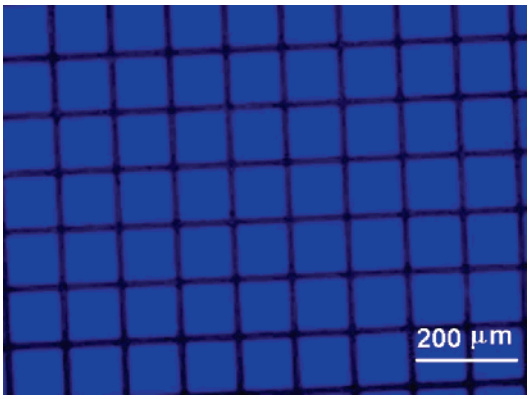

Figure 9. Fluorescent photoimage generated by photooxidation of **P2** (sample from Table 2, no. 5). The photograph was taken under a fluorescence optical microscope.

(1) The nonmesomorphic monomers are prepared by multistep reaction routes and polymerized by WCl_6-Ph_4Sn catalyst. The resulting polymers show high thermal stability and start to lose their weights at temperatures as high as ≥400 °C, thanks to the protective jacket effect contributed by the thermally stable aromatic pendants.

(2) Except for **P1**, **P2** and **P3** are liquid crystalline and form a monolayered S_A mesophase at high temperatures. The functional bridge group is found to affect the packing arrangements of the mesogenic pendants in the mesophases.

(3) All the polymers are emissive. Upon photoexcitation, the polymers emit strong blue and blue-green lights of 460 and 480 nm, respectively, in high quantum efficiency (>30%). The functional bridge group linked to the backbone phenyl ring affects the peak maximum, with the emission of **P3** being 18 nm red-shifted from those of **P1** and **P2**.

(4) The polymers are sensitive to photooxidation, although they are photochemically stable in the inert atmosphere. UV irradiation of a thin film of **P2** in air through a mask selectively oxidizes the exposed regions and quenches their light emissions, furnishing a well-resolved, luminescent pattern.

Conjugated polymers carrying biphenyl appendages are promising materials for nonlinear optics.[21] Unlike vinyl polymers, the backbones of our acetylenic polymers are π-conjugated. It is envisioned that the new polymers may have an array of potential applications in optoelectronic and quantum electronic systems.

Experimental Section

Materials. Toluene (BDH) was predried over 4 Å molecular sieves and distilled under nitrogen from sodium benzophenone ketyl immediately prior to use. Dichloromethane (Lab-Scan) was dried over molecular sieves and distilled under nitrogen over calcium hydride. Except for molybdenum(V) chloride (Acros), all other reagents and solvents were purchased from Aldrich and used as received without further purification. Compounds 4′-hydroxy-4-biphenylyl heptyl ether (**13**) and 4′-heptyloxyl-4-biphenylcarboxylic acid (**15**) were prepared according to our previously published procedures.[8d]

Instrumentation. The ^1H and ^{13}C NMR spectra were recorded on a Bruker ARX 300 NMR spectrometer using chloroform-*d* as solvent and tetramethylsilane ($\delta = 0$) or chloroform ($\delta = 7.26$) as internal reference. The mass spectra were recorded on a Finnigan TSQ 7000 triple quadrupole mass spectrometer operating in a chemical ionization (CI) mode using methane as carrier gas. The molecular weights of the polymers were estimated by a Waters Associates GPC system. Degassed THF was used as eluent at a flow rate of 1.0 mL/min. A set of monodisperse polystyrene standards covering the molecular weight range of 10^3-10^7 was used for the molecular weight calibration.

The UV absorption spectra were measured on a Milton Roy Spectronic 3000 Array spectrophotometer, and the molar absorptivity (ϵ) of the polymers was calculated on the basis of their monomer repeat units. The PL spectra were recorded in THF on an SLM 8000C spectrofluorometer. The quantum yields of the polymers in THF were measured using the literature procedures.[22] Both the polymer and reference (9,10-diphenylanthracene) solutions were excited at the same wavelengths to avoid the possible error caused by neglecting the difference between the excitation light intensities of different wavelengths. The quantum yield for 9,10-diphenylanthracene in cyclohexane was assumed to be 90%.

The thermal stability of the polymers was evaluated on a Perkin-Elmer TGA 7 under nitrogen at a heating rate of 20 °C/min. A Perkin-Elmer DSC 7 was employed to measure the phase transition thermograms. An Olympus BX 60 POM equipped with a Linkam TMS 92 hot stage was used to observe anisotropic optical textures. The XRD patterns were recorded on a Philips PW1830 powder diffractometer with a graphite monochromator using 1.5406 Å Cu Kα wavelength at room temperature (scanning rate: 0.05°/s, scan range 2−30°). The polymer samples for the XRD measurements were prepared by freezing the molecular arrangements in the liquid-crystalline states by liquid nitrogen as previously reported.[8f]

Photooxidation of the polymer film was conducted in air at room temperature (~23 °C) for 2 min using 365 nm UV light with an intensity of ~30 mW/cm^2. The polymer film was prepared by spin-coating the polymer solution (~2 wt % in 1,2-dichloroethane) at 2000 rpm for 1 min on a silicon wafer. The film was dried in a vacuum oven at room temperature overnight. The fluorescence imaging was generated using a Cu-negative mask and taken on a fluorescent optical microscopy (Olympus BX4) using a broad-range UV source (330−385 nm).

Monomer Synthesis. The mesogen-containing 1-phenyl-1-alkynes (**1**−**3**) were prepared by multistep reactions according to the synthetic routes given in Schemes 1−3. Typical procedures for the synthesis of the monomers are given below.

4-(12-Bromododecyloxy)iodobenzene (11). In a 500 mL Erlenmeyer flask equipped with a condenser were dissolved 4.3 g (19.3 mmol) of 4-iodophenol (**10**) and 1.1 g of KOH (19.5 mmol) in 200 mL of acetone/DMSO mixture (10:1 by volume)

under gentle heating and stirring. To the homogeneous solution were added 6.4 g (19.4 mmol) of 1,12-dibromododecane and a catalytic amount of potassium iodide. The resulting mixture was then refluxed for 24 h. The reaction mixture was poured into 200 mL of water and acidified with 10 mL of 37% hydrochloric acid. The precipitate was collected by suction filtration. The crude product was purified on a silica gel column using chloroform/hexane mixture (1:3 by volume) as eluent. White solid; yield 41.7%.

1-[4-(12-Bromododecyl)phenyl]-1-octyne (12). To a 250 mL two-necked flask were added 0.12 g (0.17 mmol) of $PdCl_2(PPh_3)_2$, 0.1 mg (0.1 mmol) of CuI, and 150 mL of a triethylamine solution of **11** (4.0 g, 8.6 mmol) under nitrogen. After all the catalysts were dissolved, 1.5 mL of 1-octyne (10.2 mmol) was injected into the flask and the mixture was stirred at 60 °C for 24 h. After filtering out the formed salt, the solution was concentrated by a rotary evaporator. The product was purified by a silica gel column using chloroform/hexane (1:1 by volume) as eluent. Pale yellow solid; yield 79.3%.

1-[4-({[(4′-Heptyloxy-4-biphenylyl)oxy]dodecyl}oxy)phenyl]-1-octyne (1). This monomer was prepared by etherification of **12** with 4′-hydroxy-4-biphenylyl heptyl ether (**13**), using the procedures similar to those for the preparation of **11**. Purification of the monomer was achieved by silica gel chromatography, using chloroform/hexane mixture (1:2 by volume) as eluent, followed by recrystallization from absolute ethanol. White solid; yield 56.4%. ^{1}H NMR (300 MHz, $CDCl_3$), δ (ppm): 7.45 [d, 4H, Ar−H meta to OC_7H_{15} and $O(CH_2)_{12}$], 7.30 (d, 2H, Ar−H ortho to C≡C), 6.93 [d, 4H, Ar−H ortho to OC_7H_{15} and $O(CH_2)_{12}$], 6.80 (d, 2H, Ar−H meta to C≡C), 3.95 (m, 6H, OCH_2), 2.38 (t, 2H, ≡C−CH_2), 1.77 (m, 6H, OCH_2CH_2), 1.46−1.30 [m, 24 H, $(CH_2)_{12}$], 0.90 [t, 6H, $(CH_3)_2$]. ^{13}C NMR (75 MHz, $CDCl_3$), δ (ppm): 158.5 (aromatic carbons para to C≡C), 158.2 [aromatic carbons linked with OC_7H_{15} and $O(CH_2)_{12}$], 133.3 [aromatic carbons para to OC_7H_{15} and $O(CH_2)_{12}$], 132.8 (aromatic carbons ortho to C≡C), 127.6 [aromatic carbons meta to OC_7H_{15} and $O(CH_2)_{12}$], 116.0 (aromatic carbon linked with C≡C), 114.7 [aromatic carbons ortho to OC_7H_{15} and $O(CH_2)_{12}$], 114.3 (aromatic carbons meta to C≡C), 88.8 (≡CCH_2), 80.3 (ArC≡), 68.1 (OCH_2), 31.8, 31.4, 29.6, 29.4, 29.3, 29.2, 29.1, 28.9, 28.6, 26.06, 26.03, 26.00, 22.62, 22.57, 19.4 (≡CCH_2), 14.09, 14.07. MS (CI): *m*/*e* 653.1 [$(M + 1)^+$, calcd 653.1].

4-(11-Hydroxylundecyloxy)iodobenzene (14). This compound was synthesized by etherification of 4-iodophenol with 11-bromo-1-undecanol according to the procedure described above. The crude product was purified by recrystallization in absolute ethanol. White solid; yield 72.6%.

4-(11-{[4′-Heptyloxy-4-biphenylyl)carbonyl]oxy}undecyloxy)iodobenzene (11). 4′-Heptyloxy-4-biphenylcarboxylic acid (**15**; 1.3 g, 4.2 mmol), **14** (1.6 g, 4.2 mmol), TsOH (0.14 g, 0.8 mmol), and DMAP (0.1 g, 0.8 mmol) were dissolved in 100 mL of dry dichloromethane in a 500 mL two-necked flask under nitrogen. The solution was cooled to 0−5 °C with an ice-bath, to which 1.3 g of DCC (6.3 mmol) in 50 mL of dichloromethane was added under stirring via a dropping funnel with a pressure-equalization arm. The mixture was stirred at room temperature overnight. After filtering out the formed insoluble urea crystals, the filtrate was concentrated by a rotary evaporator. The crude product was purified by a silica gel column using chloroform as eluent. Recrystallization from absolute ethanol gave 2.5 g (89.0%) of a white solid.

1-{4-[({[(4′-Heptyloxy-4-biphenylyl)carbonyl]oxy}undecyl)oxy]phenyl}-1-octyne (2). This monomer was obtained by coupling reaction of **16** with 1-octyne, according to the procedures used for the preparation of **12**. White solid; yield 66.0%. ^{1}H NMR (300 MHz, $CDCl_3$), δ (ppm): 8.07 [d, 2H, Ar−H ortho to CO_2], 7.60 (d, 2H, Ar−H meta to CO_2), 7.53 (d, 2H, Ar−H meta to OC_7H_{15}), 7.29 (d, 2H, Ar−H ortho to C≡C), 6.97 (d, 2H, Ar−H ortho to OC_7H_{15}], 6.78 (d, 2H, Ar−H meta to C≡C), 4.32 (t, 2H, CH_2OCO), 3.98 (t, 2H, $OCH_2C_6H_{13}$), 3.91 [t, 2H, $OCH_2(CH_2)_{11}$], 2.37 (t, 2H, ≡C−CH_2), 1.77 (m, 6H, OCH_2CH_2), 1.46−1.31 [m, 22H, $(CH_2)_{11}$], 0.90 [t, 6H, $(CH_3)_2$]. ^{13}C NMR (75 MHz, $CDCl_3$), δ (ppm): 166.6 (CO), 159.4 (aromatic carbon linked with OC_7H_{15}), 158.5 (aromatic carbons para to C≡C), 145.2 (aromatic carbons para to CO_2), 132.8 (aromatic carbons ortho to C≡C), 132.1 (aromatic carbons para to OC_7H_{15}), 130.0 (aromatic carbons ortho to CO_2), 128.5 (aromatic carbons meta to OC_7H_{15}), 126.4 (aromatic carbons meta to CO_2), 116.0 (aromatic carbon linked with C≡C), 114.9 (aromatic carbons ortho to OC_7H_{15}), 114.3 (aromatic carbons meta to C≡C), 88.7 (≡CCH_2), 80.3 (ArC≡), 68.1 ($OCH_2C_6H_{13}$), 67.96 [$OCH_2(CH_2)_{10}$], 65.1 ($COOCH_2$), 31.8, 31.4, 29.5, 29.4, 29.3, 29.2, 29.1, 28.9, 28.7, 28.6, 26.05, 26.00, 22.62, 22.57, 19.4 (≡CCH_2), 14.09. MS (CI): *m*/*e* 671.1 [$(M + 1)^+$, calcd 671.1].

1-[(4-Methoxycarbonyl)phenyl]-1-octyne (18). This compound was prepared by coupling reaction of methyl 4-bromobenzoate with 1-octyne. The procedures were similar to those for the preparation of **12**. Pale yellow liquid; yield 92.0%.

1-[(4-Hydroxylcarbonyl)phenyl]-1-octyne (19). In a 500 mL round-bottom flask equipped with a condenser were placed 5.0 g (20.5 mmol) of **18** and 150 mL of 4% (w/v) ethanol solution of KOH. The contents were then refluxed for 4 h. The mixture was poured into 300 mL of 1 M HCl. The product was collected by suction filtration and dried under vacuum. Pale brown solid; yield 91.6%.

1-[4-(12-Hydroxyldodecyloxycarbonyl)phenyl]-1-octyne (20). This compound was prepared by esterification of **19** with 1,12-dodecanediol in the presence of DCC, TsOH, and DMAP. Purification of the crude product was achieved by a silica gel column, using chloroform/acetone (10:1 by volume) as eluent. White solid; yield 68.6%.

1-(4-{[({[(4′-Heptyloxy-4-biphenylyl)carbonyl]oxy}dodecyl)oxy]carbonyl}phenyl)-1-octyne (3). This monomer was obtained from the reaction of **20** with **15**, again using DCC as the dehydrating agent. The crude product was purified first by silica gel chromatography, using chloroform as eluent, followed by recrystallization in absolute ethanol. White solid; yield 72.7%. ^{1}H NMR (300 MHz, $CDCl_3$), δ (ppm): 8.07 (d, 2H, Ar−H meta to $ArOC_7H_{15}$), 7.94 (d, 2H, Ar−H meta to C≡C), 7.62 (d, 2H, Ar−H ortho to $ArOC_7H_{15}$), 7.57 (d, 2H, Ar−H meta to OC_7H_{15}), 7.54 (d, 2H, Ar−H ortho to C≡C), 6.97 (d, 2H, Ar−H ortho to OC_7H_{15}), 4.32 (m, 4H, CH_2OCO), 4.00 (t, 2H, OCH_2), 2.42 (t, 2H, ≡C−CH_2), 1.78 (m, 6H, CH_2CH_2OCO and OCH_2CH_2), 1.48−1.29 [m, 24H, $(CH_2)_{12}$], 0.90 [t, 6H, $(CH_3)_2$]. ^{13}C NMR (75 MHz, $CDCl_3$), δ (ppm): 166.2 (OCAr−Ar), 165.8 (≡C−ArCO), 159.2 (aromatic carbon linked with OC_7H_{15}), 144.9 (aromatic carbon linked with $ArOC_7H_{15}$), 131.8 (aromatic carbons para to OC_7H_{15}), 131.2 (aromatic carbons ortho to C≡C), 129.8 (aromatic carbons meta to $ArOC_7H_{15}$), 129.1 (aromatic carbons meta to C≡C), 129.0 (aromatic carbons para to C≡C), 128.7 (aromatic carbon linked with C≡C), 128.3 (aromatic carbons meta to OC_7H_{15}), 128.0 (aromatic carbons para to $ArOC_7H_{15}$), 126.1 (aromatic carbons ortho to $ArOC_7H_{15}$), 114.7 (aromatic carbons ortho to OC_7H_{15}), 93.6 (≡CCH_2), 80.6 (ArC≡), 67.8 (OCH_2), 65.0 (CH_2OCOAr−Ar), 64.8 (≡$CArCO_2CH_2$), 31.6, 31.2, 29.4, 29.14, 29.12, 28.9, 28.6, 28.53, 28.45, 28.40,

25.90, 25.86, 22.47, 22.38, 19.3 (≡C−*C*H_2), 13.93, 13.88. MS (CI): *m/e* 709.1 [(M + 1)$^+$, calcd 709.1].

Polymerization. All the polymerization reactions and manipulations were carried out under nitrogen using Schlenk techniques in a vacuum line system or an inert-atmosphere glovebox (Vacuum Atmospheres), except for the purification of the polymers, which was done in an open atmosphere. Typical experimental procedures for the polymerization of **1** are given below.

Into a baked 20 mL Schlenk tube with a stopcock in the sidearm was added 203 mg (0.3 mmol) of **1**. The tube was evacuated under vacuum and then flushed with dry nitrogen three times through the sidearm. Freshly distilled toluene (1 mL) was injected into the tube to dissolve the monomer. The catalyst solution was prepared in another tube by dissolving 8.0 mg of tungsten(VI) chloride and 9.0 mg of tetraphenyltin in 1 mL of toluene. The two tubes were aged at 60 °C for 15 min, and the monomer solution was transferred to the catalyst solution using a hypodermic syringe. The reaction mixture was stirred at room temperature under nitrogen for 24 h. The solution was then cooled to room temperature, diluted with 10 mL of chloroform, and added dropwise to 500 mL of acetone/chloroform mixture (10:1 by volume) through a cotton filter under stirring to remove insoluble, if any, materials. The precipitate was allowed to stand overnight and was then filtered with a Gooch crucible. The polymer was washed with acetone and dried in a vacuum oven to a constant weight.

Characterization Data for Poly{1-[4-({[(4′-heptyloxy-4-biphenylyl)oxy]dodecyl}oxy)phenyl]-1-octyne} (P1). Brown solid; yield 86.5% (Table 1, no. 3). M_w 25 000; M_w/M_n 1.6 (GPC, polystyrene calibration). ^{1}H NMR (300 MHz, $CDCl_3$), δ (ppm): 7.47 [Ar−H meta to OC_7H_{15} and $O(CH_2)_{12}$], 6.95 [Ar−H ortho to OC_7H_{15} and $O(CH_2)_{12}$], 6.55 (Ar−H ortho and meta to C═C), 3.98 (OCH_2), 1.81 (OCH_2CH_2), 1.47−1.34 [$(CH_2)_{12}$], 0.93 [$(CH_3)_2$]. ^{13}C NMR (75 MHz, $CDCl_3$), δ (ppm): 158.2 [aromatic carbons linked with OC_7H_{15} and $O(CH_2)_{12}$], 133.3 [aromatic carbons para to OC_7H_{15} and $O(CH_2)_{12}$], 127.6 [aromatic carbons meta to OC_7H_{15} and $O(CH_2)_{12}$], 114.7 [aromatic carbons ortho to OC_7H_{15} and $O(CH_2)_{12}$], 68.1 (OCH_2), 31.8, 29.7, 29.3, 29.1, 26.1, 26.0, 22.6, 14.0. UV (THF, 5.5×10^{-5} mol/L), $\lambda_{max}/\epsilon_{max}$: 268 nm/$3.10 \times 10^4$ mol^{-1} L cm^{-1}.

Poly(1-{4-[({[(4′-Heptyloxy-4-biphenylyl)carbonyl]oxy}-undecyl)oxy]phenyl}-1-octyne) (P2). Pale brown solid; yield 19.2% (Table 2, no. 5). M_w 30 400; M_w/M_n 2.0 (GPC, polystyrene calibration). ^{1}H NMR (300 MHz, $CDCl_3$), δ (ppm): 8.07 [Ar−H ortho to CO_2], 7.59 (Ar−H meta to CO_2), 7.54 (Ar−H meta to OC_7H_{15}), 6.97 (Ar−H ortho to OC_7H_{15}), 6.45 (Ar−H ortho and meta to C═C), 4.31 (CH_2OCO), 3.98 ($OCH_2C_6H_{13}$), 3.85 [$OCH_2(CH_2)_{11}$], 1.79 (OCH_2CH_2), 1.33 [$(CH_2)_{11}$], 0.91 [$(CH_3)_2$]. ^{13}C NMR (75 MHz, $CDCl_3$), δ (ppm): 166.3 (CO), 159.1 (aromatic carbons linked with OC_7H_{15}), 144.9 (aromatic carbons para to CO_2), 131.9 (aromatic carbons para to OC_7H_{15}), 129.8 (aromatic carbons ortho to CO_2), 128.3 (aromatic carbons meta to OC_7H_{15}), 126.1 (aromatic carbons meta to CO_2), 114.7 (aromatic carbons ortho to OC_7H_{15}), 68.1 ($OCH_2C_6H_{13}$), 65.1 [$OCH_2(CH_2)_{10}$ and $COOCH_2$], 31.9, 29.8, 29.5, 29.4, 29.2, 28.9, 26.2, 26.1, 22.8, 14.3. UV (THF, 5.7×10^{-5} mol/L), $\lambda_{max}/\epsilon_{max}$: 296 nm/$2.36 \times 10^4$ mol^{-1} L cm^{-1}.

Poly[1-(4-{[({[(4′-Heptyloxy-4-biphenylyl)carbonyl]oxy}-dodecyl)oxy]carbonyl}phenyl)-1-octyne] (P3). Greenish-yellow solid; yield 26.2% (Table 2, no. 8). M_w 8200; M_w/M_n 1.8 (GPC, polystyrene calibration). ^{1}H NMR (300 MHz, $CDCl_3$), δ (ppm): 8.07 (Ar−H meta to $ArOC_7H_{15}$ and meta to C═C), 7.60 (Ar−H ortho to $ArOC_7H_{15}$), 7.54 (Ar−H meta to OC_7H_{15} and ortho to C═C), 6.97 (Ar−H ortho to OC_7H_{15}), 4.32 (CH_2-OCO), 3.99 (OCH_2), 1.79 (CH_2CH_2OCO and OCH_2CH_2), 1.33 [$(CH_2)_{12}$], 0.91 [$(CH_3)_2$]. ^{13}C NMR (75 MHz, $CDCl_3$), δ (ppm): 166.5 (OCAr−Ar), 165.6 (═C−ArCO), 159.4 (aromatic carbons linked with OC_7H_{15}), 145.1 (aromatic carbon linked with $ArOC_7H_{15}$), 132.0 (aromatic carbons para to OC_7H_{15}), 130.0 (aromatic carbons meta to $ArOC_7H_{15}$), 128.5 (aromatic carbons meta to OC_7H_{15}), 128.2 (aromatic carbons para to $ArOC_7H_{15}$), 126.3 (aromatic carbons ortho to $ArOC_7H_{15}$), 114.9 (aromatic carbons ortho to OC_7H_{15}), 68.1 (OCH_2), 65.0 (CH_2-OCOAr−Ar and ═$CArCO_2CH_2$), 31.7, 29.6, 29.3, 29.0, 28.8, 26.0, 23.6, 14.0. UV (THF, 5.6×10^{-5} mol/L), $\lambda_{max}/\epsilon_{max}$: 295 nm/$2.73 \times 10^4$ mol^{-1} L cm^{-1}.

Acknowledgment. This project was partially supported by the Research Grants Council of Hong Kong (602706, HKU2/05C, 603505, 603304, and 664903) and the Ministry of Science and Technology of China (2002CB613401). B.Z.T. is thankful for the support of the Cao Guangbiao Foundation of the Zhejiang University.

References and Notes

(1) (a) *Liquid-Crystalline Polymers*; Weiss, R. A., Ober, C. K., Eds.; American Chemical Society: Washington, DC, 1990. (b) *Liquid Crystalline Polymer Systems: Technological Advances*; Lsayev, A. I., Kyu, T., Cheng, S. Z. D., Eds.; American Chemical Society: Washington, DC, 1996. (c) *Optical Effects in Liquid Crystals*; Janossy, I., Ed.; Kluwer: Dordrecht, The Netherlands, 1991. (d) Petty, M. C.; Bryce, M. R.; Bloor, D. *An Introduction to Molecular Electronics*; Edward Arnold: London, 1995. (e) *Polymeric Liquid Crystals*; Blumstein, A., Ed.; Plenum: New York, 1985.

(2) (a) Burn, P. L.; Holmes, A. B.; Kraft, A.; Bradley, D. D. C.; Brown, A. R.; Friend, R. H. *J. Chem. Soc., Chem. Commun*. **1992**, 32. (b) Burn, P. L.; Holmes, A. B.; Kraft, A.; Bradley, D. D. C.; Brown, A. R.; Friend, R. H.; Gymer, R. W. *Nature* **1992**, *356*, 47. (c) Burroughs, J. H.; Bradley, D. D. C.; Brown, A. R.; Marks, R. N.; Mackey, K.; Friend, R. H.; Burn, P. L.; Holmes, A. B. *Nature* **1990**, *347*, 539. (d) Braun, D.; Heeger, A. J. *Appl. Phys. Lett*. **1991**, *58*, 1982. (e) Gustafsson, G.; Cao, Y.; Treacy, G. M.; Klavetter, F.; Colaneri, N.; Heeger, A. J. *Nature* **1992**, *357*, 477. (f) Friend, R. H.; Gymer, R. W.; Holmes, A. B.; Burroughes, J. H.; Marks, R. N.; Taliani, C.; Bradley, D. D. C.; Dos Santos, D. A.; Bredas, J. L.; Logdlund, M.; Salaneck, W. R. *Nature* **1999**, *397*, 121−128.

(3) (a) Shirakawa, H.; Lousi, E. J.; MacDiarmid, A. G.; Chiang, C. K.; Heeger, A. J. *J. Chem. Soc., Chem. Commun*. **1977**, 578. (b) Shirakawa, H. *Angew. Chem., Int. Ed*. **2001**, *40*, 2575−2580. (c) MacDiarmid, A. G. *Angew. Chem., Int. Ed*. **2001**, *40*, 2581−2590. (d) Heeger, A. J. *Angew. Chem., Int. Ed*. **2001**, *40*, 2591−2611.

(4) (a) Chien, J. C. W. *Polyacetylenes*; Academic: New York, 1984. (b) *Handbook of Conducting Polymers*; Skotheim, T. A., Ed.; Marcel Dekker: New York, 1986. (c) Krivoshei, I. V.; Skorobogatov, V. M. *Polyacetylenes and Polyarylenes: Synthesis and Conducting Properties*; Gordon and Breach Science: New York, 1991.

(5) (a) Lam, J. W. Y.; Tang, B. Z. *Acc. Chem. Res.* **2005**, *38*, 745−754. (b) Lam, J. W. Y.; Tang, B. Z. *J. Polym. Sci., Part A: Polym. Chem.* **2003**, *41*, 2607−2629. (c) Lam, J. W. Y.; Chen, J.; Law, C. C. W.; Peng, H.; Xie, Z.; Cheuk, K. K. L.; Kwok, H. S.; Tang, B. Z. *Macromol. Symp.* **2003**, *196*, 289−300. (d) Xie, Z.; Peng, H.; Lam, J. W. Y.; Chen, J.; Zheng, Y.; Qiu, C.; Kwok, H. S.; Tang, B. Z. *Macromol. Symp.* **2003**, *195*, 179−184. (e) Cheuk, K. K. L.; Li, B. S.; Tang, B. Z. *Curr. Trends Polym. Sci.* **2002**, *7*, 41−55. (f) Tang, B. Z. *Polym. News* **2001**, *26*, 262−272.

(6) (a) Masuda, T.; Higashimura, T. *Adv. Polym. Sci.* **1987**, *81*, 121. (b) Yashima, E.; Maeda, K.; Nishimura, T. *Chem. Eur. J*. **2004**, *10*, 43−51. (c) Sedlacek, J.; Vohlidal, J. *Collect. Czech. Chem. Commun*. **2003**, *68*, 1745−1790. (d) Nagai, K.; Masuda, T.; Nakagawa, T.; Freeman, B. D.; Pinnau, Z. *Prog. Polym. Sci*. **2001**, *26*, 721−798. (e) Choi, S. K.; Gal, Y. S.; Jin, S. H.; Kim, H. K. *Chem. Rev*. **2000**, *100*, 1645−1681. (f) Saunders, R. S.; Cohen, R. E.; Schrock, R. R. *Acta Polym*. **1994**, *45*, 301−307. (g) Nakano, T.; Okamoto, Y. *Chem. Rev*. **2001**, *101*, 4013.

(7) (a) Scherman, O. A.; Rutenberg, I. M.; Grubbs, R. H. *J. Am. Chem. Soc*. **2003**, *125*, 8515−8522. (b) Percec, V.; Obata, M.; Rudick, J. G.; De, B. B.; Glodde, M.; Bera, T. K.; Magonov, S. N.; Balagurusamy, V. S. K.; Heiney, P. A. *J. Polym. Sci., Part A: Polym. Chem.* **2002**, *40*, 3509−3533. (c) Shinohara, K.; Aoki, T.; Kanek, T. *J. Polym. Sci., Part A: Polym. Chem.* **2002**, *40*, 1689−1697. (d) Safir, A. L.; Novak, B. M. *Macromolecules* **1993**,

26, 4072−4073. (e) Moore, J. S.; Gorman, C. B.; Grubbs, R. H. *J. Am. Chem. Soc*. **1991**, *113*, 1704−1712.

(8) (a) Lam, J. W. Y.; Dong, Y.; Luo, J.; Cheuk, K. K. L.; Xie, Z.; Kwok, H. S.; Tang, B. Z. *Thin Solid Films* **2002**, *417*, 143−146. (b) Lam, J. W. Y.; Dong, Y.; Cheuk, K. K. L.; Luo, J. D.; Xie, Z.; Kwok, H. S.; Mo, Z.; Tang, B. Z. *Macromolecules* **2002**, *35* (4), 1229−1240. (c) Mi, Y. L.; Tang, B. Z. *Polym. News* **2001**, *26*, 170. (d) Lam, J. W. Y.; Kong, X.; Dong, Y. P.; Cheuk, K. K. L.; Xu, K.; Tang, B. Z. *Macromolecules* **2000**, *33*, 5027−5040. (e) Kong, X.; Lam, J. W. Y.; Tang, B. Z. *Macromolecules* **1999**, *32*, 1722−1730. (f) Kong, X.; Tang, B. Z. *Chem. Mater*. **1998**, *10*, 3352−3363. (g) Tang, B. Z.; Kong, X.; Wan, X.; Peng, H.; Lam, W. Y.; Feng, X.; Kwok, H. S. *Macromolecules* **1998**, *31*, 2419−2432. (h) Geng, J.; Zhao, X.; Zhou, E.; Li, G.; Lam, J. W. Y.; Tang, B. Z. *Mol. Cryst. Liq. Cryst*. **2003**, *399*, 17−28. (i) Lam, J. W. Y.; Law, C. K.; Dong, Y.; Wang, J.; Ge, W.; Tang, B. Z. *Opt. Mater*. **2002**, *21*, 321−324.

(9) (a) Schenning, A. P. H. J.; Fransen, M.; Meijer, E. W. *Macromol. Rapid. Commun*. **2002**, *23* (4), 266−270. (b) Ting, C. H.; Chen, J. T.; Hsu, C. S. M*acromolecules* **2002**, *35* (4), 1180−1190. (c) Stagnaro, P.; Cavazza, B.; Trefiletti, V.; Costa, G.; Gallot, B.; Valenti, B. *Macromol. Chem. Phys*. **2001**, *202*, 2065−2073. (d) Gui, T. L.; Jin, S. H.; Park, J. W.; Ahn, W. S.; Koh, K. N.; Kim, S. H.; Gal, Y. S. *Opt. Mater.* **2003**, *21*, 637−641. (e) Karoda, H.; Goto, H.; Akagi, K.; Kawaguchi, A. *Macromolecules* **2002**, *35*, 1307−1313.

(10) (a) Koltzenburg, S.; Stelzer, F.; Nuyken, O. *Macromol. Chem. Phys.* **1999**, *200*, 821−827. (b) Koltzenburg, S.; Wolff, P.; Stelzer, F.; Springer, J.; Nuyken, O. *Macromolecules* **1998**, *31*, 9166−9173. (c) Le Moigne, J.; Hilberer, A.; Kajazan, F. *Makromol. Chem*. **1992**, *193*, 515. (d) Karoda, H.; Goto, H.; Akagi, K.; Kawaguchi, A. *Macromolecules* **2002**, *35*, 1307−1313.

(11) (a) Masuda, T.; Tang, B. Z.; Higashimura, T.; Yamaoka, H. *Macromolecules* **1985**, *18*, 2369−2373. (b) Masuda, T.; Tang, B. Z.; Tanaka, T.; Higashimura, T. *Macromolecules* **1986**, *19*, 1459−1464. (c) Sun, R.; Masuda, T.; Kobayashi, T. *Synth. Met.* **1997**, *91*, 301−303. (d) Sun, R.; Zheng, Q.; Zhang, X.; Masuda, T.; Kobayashi, T. *Jpn. J. Appl. Phys.* **1999**, *38*, 2017−2023. (e) Chen, J.; Xie, Z.; Lam, J. W. Y.; Law, C. C. W.; Tang, B. Z. *Macromolecules* **2003**, *36*, 1108−1117.

(12) (a) Lam, J. W. Y.; Luo, J.; Dong, Y.; Cheuk, K. K. L.; Tang, B. Z. *Macromolecules* **2002**, *35*, 8288−8299. (b) Dong, Y.; Lam, J. W. Y.; Peng, H.; Kwok, H. S.; Tang, B. Z. *Macromolecules* **2004**, *37*, 6408−6417. (c) Lam, J. W. Y.; Dong, Y.; Kwok, H.; Shen, J. C.; Tang, B. Z. *Macromolecules* **2005**, *38*, 3290−3300.

(13) (a) McArdle, C. B. *Side Chain Liquid Crystal Polymers*; Blackie: London, 1989. (b) *Handbook of Liquid Crystal Research*; Collings, P. J., Patel, J. S., Eds.; Oxford University Press: New York, 1997.

(14) (a) Tabata, M.; Sone, T.; Sadahiro, Y. *Macromol. Chem. Phys.* **1999**, *200*, 265−282. (b) Reddinger, J. L.; Reynolds, J. R. *Adv. Polym. Sci*. **1999**, *145*, 57−122. (c) Masuda, T.; Takahashi, T.; Higashimura, T. *Macromolecules* **1985**, *18*, 311−317. (d) Ginsburg, E. J.; Gorman, C. B.; Grubbs, R. H. In *Modern Acetylene Chemistry*; Stang, P. J., Diederich, F., Eds.; VCH: New York, 1995; Chapter 10, pp 353−383.

(15) (a) Seki, H.; Tang, B. Z.; Tanaka, A.; Masuda, T. *Polymer* **1994**, *35*, 3456−3462. (b) Karim, S. M.; Nomura, R.; Masuda, T. *J. Polym. Sci., Part A: Polym. Chem.* **2001**, *39*, 3130−3136.

(16) (a) Percec, V.; Pugh, C. In *Side Chain Liquid Crystal Polymers*; McArdle, C. B., Ed.; Chapman & Hall: New York, 1989; Chapter 3, pp 30−105. (b) Pugh, C.; Kiste, A. L. *Prog. Polym. Sci*. **1997**, *22*, 601−691. (c) Shiota, A.; Ober, C. K. *Prog. Polym. Sci*. **1997**, *22*, 975−1000.

(17) *Liquid Crystalline Order in Polymers*; Blumstein, A., Hsu, E. C., Eds.; Academic Press: New York, 1978.

(18) Liu, Z.; Zhu, L.; Zhou, W.; Cheng, S. Z. D.; Percec, V.; Ungar, G. *Chem. Mater.* **2002**, *14*, 2384−2392 and references therein.

(19) Lam, J. W. Y.; Dong, Y.; Tang, B. Z. *Polym. Prepr*. **2001**, *42* (2), 508−509.

(20) Kwak, G.; Fujiki, M.; Sakaguchi, T.; Masuda, T. *Macromolecules* **2006**, *39*, 319−323.

(21) Makowska-Janusik, M.; Tkaczyk, S.; Kityk, I. V. *J. Phys. Chem. B* **2006**, *110*, 6492−6498.

(22) (a) Liao, L.; Pang, Y. *Macromolecules* **2001**, *34*, 7300−7305. (b) Osaheni, J. A.; Jenekhe, S. A. *J. Am. Chem. Soc*. **1995**, *117*, 7389−7398. (c) Demas, J. N.; Crosby, G. A. *J. Phys. Chem*. **1971**, *75*, 991. (d) Ingle, J. D.; Crouch, S. R. *Spectrochemical Analysis*; Prentice Hall: London, 1998; pp 52−55.